



# Hip Fractures in Older Adults Are Associated With the Low Density Bone Phenotype and Heterogeneous Deterioration of Bone Microarchitecture

Danielle E Whittier, Sarah L Manske, Emma Billington, Richard EA Walker, Prism S Schneider, Lauren A Burt,  David A Hanley, and Steven K Boyd 

McCaig Institute for Bone and Joint Health, Cumming School of Medicine, University of Calgary, Calgary, Canada

## ABSTRACT

Femoral neck areal bone mineral density (FN aBMD) is a key determinant of fracture risk in older adults; however, the majority of individuals who have a hip fracture are not considered osteoporotic according to their FN aBMD. This study uses novel tools to investigate the characteristics of bone microarchitecture that underpin bone fragility. Recent hip fracture patients ( $n = 108$ , 77% female) were compared with sex- and age-matched controls ( $n = 216$ ) using high-resolution peripheral quantitative computed tomography (HR-pQCT) imaging of the distal radius and tibia. Standard morphological analysis of bone microarchitecture, micro-finite element analysis, and recently developed techniques to identify void spaces in bone microarchitecture were performed to evaluate differences between hip fracture patients and controls. In addition, a new approach for phenotyping bone microarchitecture was implemented to evaluate whether hip fractures in males and females occur more often in certain bone phenotypes. Overall, hip fracture patients had notable deterioration of bone microarchitecture and reduced bone mineral density compared with controls, especially at weight-bearing sites (tibia and femoral neck). Hip fracture patients were more likely to have void spaces present at either site and had void spaces that were two to four times larger on average when compared with non-fractured controls ( $p < 0.01$ ). Finally, bone phenotyping revealed that hip fractures were significantly associated with the *low density* phenotype ( $p < 0.01$ ), with the majority of patients classified in this phenotype (69%). However, female and male hip fracture populations were distributed differently across the bone phenotype continuum. These findings highlight how HR-pQCT can provide insight into the underlying mechanisms of bone fragility by using information about bone phenotypes and identification of microarchitectural defects (void spaces). The added information suggests that HR-pQCT can have a beneficial role in assessing the severity of structural deterioration in bone that is associated with osteoporotic hip fractures. © 2022 The Authors. *Journal of Bone and Mineral Research* published by Wiley Periodicals LLC on behalf of American Society for Bone and Mineral Research (ASBMR).

**KEY WORDS:** HIGH-RESOLUTION PERIPHERAL QUANTITATIVE COMPUTED TOMOGRAPHY; BONE MICROARCHITECTURE; HIP FRACTURE; FRACTURE RISK; OSTEOPOROSIS; BONE PHENOTYPE

## Introduction

Hip fractures have a devastating impact on patients. The quality of life after a hip fracture is often greatly reduced,<sup>(1-3)</sup> and approximately one-quarter of patients die within a year.<sup>(4,5)</sup> In addition, hip fractures place a disproportionate burden on health care systems as they account for nearly half of all acute-care costs related to osteoporosis.<sup>(6)</sup> Defined as a major osteoporotic fracture, hip fractures are a result of advanced decline in bone strength, but identifying who is at risk remains a challenge. Current clinical diagnosis of osteoporosis

typically relies on femoral neck areal bone mineral density (FN aBMD) measured using dual-energy X-ray absorptiometry (DXA), where individuals with a FN aBMD  $\leq 2.5$  standard deviations (SD) below a young female reference population are considered osteoporotic.<sup>(7)</sup> However, the majority of individuals who suffer hip fractures do not have a FN aBMD below this diagnostic threshold.<sup>(8-10)</sup> The suboptimal sensitivity of FN aBMD has led to the development of clinical tools, such as the Fracture Risk Assessment Tool (FRAX), that use clinical risk factors to account for information about bone health that is not captured by FN aBMD.<sup>(11,12)</sup> However, clinical risk factors are indirect approach

This is an open access article under the terms of the [Creative Commons Attribution-NonCommercial-NoDerivs](https://creativecommons.org/licenses/by-nc-nd/4.0/) License, which permits use and distribution in any medium, provided the original work is properly cited, the use is non-commercial and no modifications or adaptations are made.

Received in original form January 25, 2022; revised form July 22, 2022; accepted July 22, 2022.

Address correspondence to: Steven K Boyd, PhD, McCaig Institute for Bone and Joint Health, University of Calgary, Room HRIC 3A16, 3280 Hospital Drive NW, Calgary, Alberta, T2N 4Z6, Canada. E-mail: [skboyd@ucalgary.ca](mailto:skboyd@ucalgary.ca)

Additional Supporting Information may be found in the online version of this article.

*Journal of Bone and Mineral Research*, Vol. 37, No. 10, October 2022, pp 1963–1972.

DOI: 10.1002/jbmr.4663

© 2022 The Authors. *Journal of Bone and Mineral Research* published by Wiley Periodicals LLC on behalf of American Society for Bone and Mineral Research (ASBMR).

to capturing bone quality, so even with tools like FRAX, stratification of fracture risk remains a challenge.

High-resolution peripheral quantitative computed tomography (HR-pQCT) is a promising alternative to identify individuals at risk of fracture by providing information about volumetric bone mineral density (BMD), microarchitecture, and biomechanical properties.<sup>(13,14)</sup> A recent meta-analysis and a prospective multicenter study have established a strong relationship between outcome measures of bone properties obtained from HR-pQCT with fragility fracture risk.<sup>(15,16)</sup> However, in these analyses, fracture sites were pooled and the proportion of hip fracture patients was relatively small, limiting the ability to identify bone characteristics intrinsic to hip fracture risk, a primary outcome of interest when determining whether clinical intervention is appropriate. Previous studies using HR-pQCT to investigate bone microarchitecture in hip fracture patients independent of other fracture types have been limited in sample size ( $n = 24-62$ ) and only included females.<sup>(17-19)</sup> In addition, recent advances in image resolution available with the second-generation HR-pQCT,<sup>(20)</sup> alongside newly introduced analytical techniques of void space analysis<sup>(21)</sup> and bone phenotyping,<sup>(22)</sup> present a unique opportunity to investigate bone characteristics of osteoporosis to improve identifying people at high risk of hip fracture.

The objective of this study was to determine the characteristics of bone microarchitecture that underpin fragility by investigating differences between patients with a recent hip fracture and healthy controls. The association between hip fracture status with bone phenotype, void spaces, and conventional morphological bone properties was assessed.

## Materials and Methods

### Participants

Females and males with a recent hip fragility fracture were recruited through the Fracture Liaison Services (FLS) program in Calgary, Canada, between June 2017 and February 2021. Participants were screened within 1 week of their fracture by an FLS nurse. Hip fracture patients were eligible if they were aged 55 years or older, at least 5 years post-menopause in the case of females, and had sustained the fracture due to a low-energy fall from 5 feet or less. Fractures were not included if they were pathologic, atypical, peri-prosthetic, or if the patient had already experienced any prior hip fracture. Patients were also ineligible if they had an active malignancy, primary hyperparathyroidism, Paget's disease, renal disease, or were being treated with strontium ranelate. Finally, patients were screened for factors that were not directly related to bone health but would impact their ability to participate in the study, including dementia or other cognitive impairments, declining health, immobility, movement disorders, travel distance, and prior fractures or surgical history that would limit the ability to acquire medical imaging. Eligible patients were invited to participate, and study visits were scheduled within 6 months of the fracture date.

A subset of participants from a previously reported population-based normative cohort were used as controls.<sup>(23)</sup> The normative population consists of 1236 adults between the ages of 18 and 95 years old and was recruited from the general population through posters, social media promotion, and snowball recruiting. Participants from the normative cohort who met the same health screening criteria as hip fracture patients were identified and controls were selected using random sampling, stratified by sex and age, to obtain a 1:2 case/control ratio.

All participants provided written informed consent before involvement in the study, and study approval was obtained from the Conjoint Health Research Ethics Board at the University of Calgary (REB16-1606).

### Anthropometric measurements and study visit questionnaires

Participants had their height and weight measured to the nearest 0.1 cm and 0.1 kg, respectively. Participant health history, medication use, and fracture history were captured using detailed questionnaires. Hip fracture patients completed an additional questionnaire providing the cause of their hip fracture, and pre- and post-fracture mobility score on a scale from 0 (no restrictions in walking or need of walking aid) to 9 (bed-bound) to capture changes in mobility due to the fracture.<sup>(24)</sup>

### Medical imaging

Femoral neck aBMD was measured using iDXA (GE Lunar Hologic, GE Healthcare, Madison, WI, USA; encore v16). The left femoral neck of controls was scanned, and in the case of patients with a left hip fracture, the non-fractured side was used.

Participants were scanned at the distal radius and tibia using second-generation HR-pQCT (XtremeCT II, Scanco Medical AG, Brütisellen, Switzerland) following the standard *in vivo* protocol.<sup>(20,25)</sup> The non-dominant radius and left tibia were scanned for all control participants. In the case of hip fracture patients, the non-dominant radius was comparably scanned; however, the tibia on the hip fracture side was selected, in alignment with previously reported protocol.<sup>(19)</sup> If there was prior fracture, surgery, or implant at the HR-pQCT scan site, the contralateral side was scanned. A subset of hip fracture patients were additionally scanned at the tibia on the non-fracture side to determine if asymmetrical bone loss occurs due to unloading of the fracture side during recovery. The scan reference line was placed at the endplate of the distal radius or tibia, and scan acquisition began at a fixed-offset proximal from the reference line of 9.5 and 22.5 mm, for the radius and tibia, respectively. Each scan consisted of 168 slices (10.2 mm) with a nominal isotropic resolution of 61  $\mu\text{m}$ . Scans were graded for motion artifacts from a scale of 1 (no motion) to 5 (significant blurring and discontinuities), and scores of 4 or higher were excluded from analysis.<sup>(26)</sup>

### HR-pQCT analysis

Image analysis followed the manufacturer's standard patient evaluation protocol.<sup>(20,25)</sup> The periosteal and endocortical contours were automatically generated using a dual-threshold technique.<sup>(27)</sup> Contours were inspected and manually corrected where necessary, following previously reported recommendations,<sup>(28)</sup> and the resulting BMD and morphological parameters were obtained: volumetric BMD of the total, cortical, and trabecular regions (Tt.BMD, Ct.BMD, and Tb.BMD, respectively); mean total, cortical, and trabecular cross-sectional areas (Tt.Ar, Ct.Ar, and Tb.Ar, respectively); trabecular bone volume fraction (Tb.BV/TV), thickness (Tb.Th), separation (Tb.Sp), number (Tb.N), and inhomogeneity (Tb.1/N.SD); and cortical thickness (Ct.Th) and porosity (Ct.Po). Void space analysis was performed on all HR-pQCT images in the trabecular bone network using a fully automated protocol<sup>(21)</sup> to determine void space-to-total volume ratio (VS/TV).

Failure load was estimated using linear micro-finite element ( $\mu$ FE) analysis on the segmented HR-pQCT images. A tissue modulus of 8748 GPa and Poisson ratio of 0.3 were used, and a linear axial compression test with 1% compressive strain was applied.<sup>(29)</sup> Failure load was estimated using the yield criterion of 2% critical volume and 0.7% critical strain,<sup>(30)</sup> and  $\mu$ FE models were solved using a conjugate gradient approach with a convergence criteria of  $1 \times 10^{-6}$  (FAIM v8.0, Numerics88 Solutions Ltd,

Calgary, Canada) on the University of Calgary's High Performance Computing cluster.

### Bone phenotyping

The bone microarchitecture phenotypes of all participants were estimated using a clustering model we recently established with the Bone Microarchitecture International Consortium (BoMIC).<sup>(22)</sup>

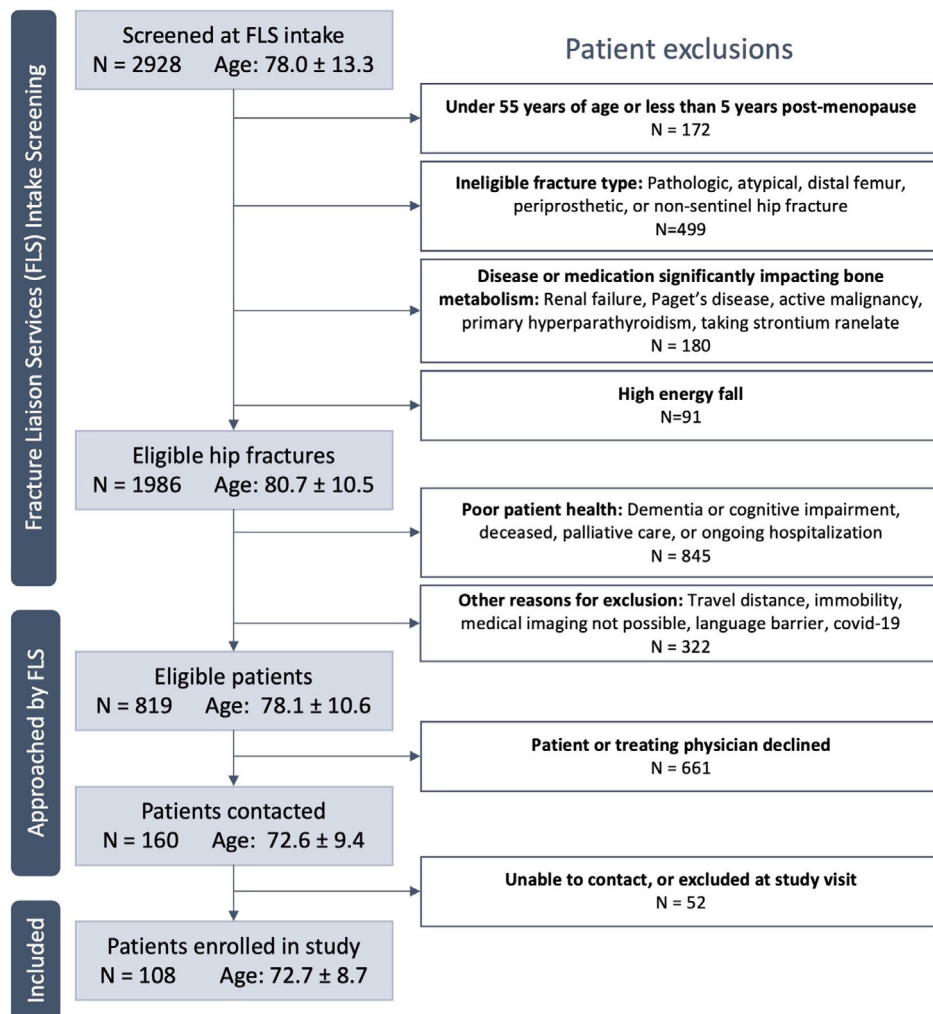


**Fig. 1.** Hip fracture patient eligibility and screening summary.

**Table 1.** Descriptive Statistics of Hip Fracture Patients and Matched Controls

	Hip fractures ( <i>n</i> = 108)	Controls ( <i>n</i> = 216)	Adjusted <i>p</i> value <sup>a</sup>
Age (years)	72.7 ± 8.7	72.1 ± 8.3	1.00
Sex (female, %)	83 (77%)	166 (77%)	1.00
Ethnicity (White, %)	101 (93.5%)	203 (94.0%)	1.00
Height (cm)	164.5 ± 9.0	163.9 ± 8.4	1.00
Weight (kg)	69.1 ± 15.6	73.4 ± 14.4	0.20
Prior fragility fracture (yes, %)	41 (38%)	49 (23%)	0.10
Osteoporosis medication >6 months (yes, %)	24 (22%)	26 (12%)	0.31

Continuous variables are presented as mean ± standard deviation, and categorical variables as frequency and ratio (%).

<sup>a</sup>The *p* values were adjusted for multiple comparisons using the Holm-Bonferroni method.

**Table 2.** Summary of Bone Parameters of the Fracture and Control Group

	Hip fractures	Controls	Difference	Adjusted <i>p</i> value <sup>a</sup>
<b>DXA</b>	<b>n = 106</b>	<b>n = 200</b>		
Femoral neck areal BMD (g/cm <sup>2</sup> )	0.74 ± 0.09	0.88 ± 0.14	<b>-16%</b>	<b>&lt;0.01</b>
Normal BMD: <i>T</i> -score > -1.0 (yes, %)	7 (7%)	78 (39%)	-	<b>&lt;0.01</b>
Low bone mass: -2.5 < <i>T</i> -score < -1.0 (yes, %)	66 (62%)	107 (54%)	-	1.00
Osteoporotic: <i>T</i> -score < -2.5 (yes, %)	33 (31%)	15 (8%)	-	<b>&lt;0.01</b>
<b>HR-pQCT—Multi-site parameters</b>	<b>n = 100</b>	<b>n = 209</b>		
Low density phenotype (yes, %)	69 (69%)	84 (40%)	-	<b>&lt;0.01</b>
Low volume phenotype (yes, %)	14 (14%)	64 (31%)	-	0.33
Healthy bone phenotype (yes, %)	17 (17%)	60 (29%)	-	<b>0.03</b>
Low density phenotype membership	0.47 ± 0.16	0.36 ± 0.19	<b>31%</b>	<b>&lt;0.01</b>
Low volume phenotype membership	0.31 ± 0.10	0.35 ± 0.14	-11%	0.74
Healthy bone phenotype membership	0.22 ± 0.16	0.29 ± 0.21	-25%	0.54
Void space at both sites (yes, %)	48 (48%)	48 (24%)	-	<b>&lt;0.01</b>
<b>HR-pQCT—Radius</b>	<b>n = 102</b>	<b>n = 209</b>		
Void space present (yes, %)	61 (60%)	82 (39%)	-	<b>0.01</b>
VS/TV (%)	6.8 ± 9.8	2.4 ± 5.8	<b>183%</b>	<b>&lt;0.01</b>
Tt.BMD (mg HA/cm <sup>3</sup> )	244.8 ± 60.1	282.8 ± 65.8	<b>-13%</b>	<b>&lt;0.01</b>
Ct.BMD (mg HA/cm <sup>3</sup> )	806.9 ± 80.4	844 ± 74.0	<b>-4%</b>	<b>&lt;0.01</b>
Tb.BMD (mg HA/cm <sup>3</sup> )	112.3 ± 44.1	137.3 ± 43.6	<b>-18%</b>	<b>&lt;0.01</b>
Tb.BV/TV (%)	15.7 ± 5.5	19.1 ± 5.9	<b>-18%</b>	<b>&lt;0.01</b>
Tb.N (mm <sup>-1</sup> )	1.083 ± 0.330	1.264 ± 0.27	<b>-14%</b>	<b>&lt;0.01</b>
Tb.Th (mm)	0.226 ± 0.018	0.228 ± 0.015	-1%	0.74
Tb.Sp (mm)	1.051 ± 0.517	0.829 ± 0.378	<b>27%</b>	<b>&lt;0.01</b>
Tb.1/N.SD (mm)	0.572 ± 0.497	0.378 ± 0.364	<b>51%</b>	<b>&lt;0.01</b>
Ct.Th (mm)	0.922 ± 0.198	0.988 ± 0.219	-7%	0.13
Ct.Po (%)	1.5 ± 0.9	1.4 ± 0.1	6%	1.00
Tt.Ar (mm <sup>2</sup> )	284.9 ± 72.7	276.9 ± 66.1	3%	1.00
Ct.Ar (mm <sup>2</sup> )	55.0 ± 14.4	57.6 ± 16.2	-4%	1.00
Tb.Ar (mm <sup>2</sup> )	233.7 ± 65.6	223.0 ± 58.0	5%	1.00
Failure load (N)	2259 ± 703	2668 ± 984	<b>-15%</b>	<b>0.02</b>
<b>HR-pQCT—Tibia</b>	<b>n = 106</b>	<b>n = 216</b>		
Void space present (yes, %)	73 (69%)	100 (46%)	-	<b>&lt;0.01</b>
VS/TV (%)	5.5 ± 7.9	1.4 ± 3.0	<b>293%</b>	<b>&lt;0.01</b>
Tt.BMD (mg HA/cm <sup>3</sup> )	209.5 ± 54.8	270.7 ± 59.0	<b>-23%</b>	<b>&lt;0.01</b>
Ct.BMD (mg HA/cm <sup>3</sup> )	698.2 ± 88.4	794 ± 87.4	<b>-12%</b>	<b>&lt;0.01</b>
Tb.BMD (mg HA/cm <sup>3</sup> )	122.8 ± 44.9	159.2 ± 40.7	<b>-23%</b>	<b>&lt;0.01</b>
Tb.BV/TV (%)	18.5 ± 5.7	23.4 ± 5.4	<b>-21%</b>	<b>&lt;0.01</b>
Tb.N (mm <sup>-1</sup> )	1.085 ± 0.31	1.267 ± 0.224	<b>-14%</b>	<b>&lt;0.01</b>
Tb.Th (mm)	0.245 ± 0.019	0.258 ± 0.024	<b>-5%</b>	<b>&lt;0.01</b>
Tb.Sp (mm)	1.066 ± 0.683	0.798 ± 0.182	<b>34%</b>	<b>&lt;0.01</b>
Tb.1/N.SD (mm)	0.633 ± 0.795	0.350 ± 0.185	<b>81%</b>	<b>&lt;0.01</b>
Ct.Th (mm)	1.262 ± 0.329	1.402 ± 0.323	<b>-10%</b>	<b>&lt;0.01</b>
Ct.Po (%)	4.5 ± 1.9	3.8 ± 1.9	<b>18%</b>	<b>0.02</b>
Tt.Ar (mm <sup>2</sup> )	742.6 ± 139.4	709.6 ± 141.0	5%	0.49
Ct.Ar (mm <sup>2</sup> )	113.1 ± 30.9	123.9 ± 33.2	-9%	0.16
Tb.Ar (mm <sup>2</sup> )	635.0 ± 132.5	591.1 ± 131.2	7%	0.07
Failure load (N)	5697 ± 1879	7536 ± 2319	<b>-24%</b>	<b>&lt;0.01</b>

DXA = dual-energy X-ray absorptiometry; BMD = bone mineral density; VS/TV = void space-to-total volume ratio; Tt.BMD = total BMD; Ct.BMD = cortical BMD; Tb.BMD = trabecular BMD; Tb.BV/TV = trabecular bone volume fraction; Tb.N = trabecular number; Tb.Th = trabecular thickness; Tb.Sp = trabecular separation; Tb.1/N.SD = trabecular inhomogeneity; Ct.Th = cortical thickness; Ct.Po = cortical porosity; Tt.Ar = total cross-sectional area; Ct.Ar = cortical cross-sectional area; Tb.Ar = trabecular cross-sectional area.

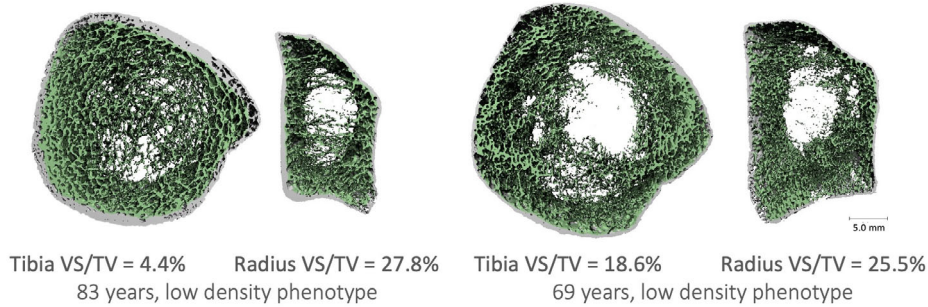
Continuous variables are in mean ± standard deviation, and categorical in frequency and ratio (%). Differences are relative to the control group, and significant differences are bolded.

<sup>a</sup>The *p* values were adjusted for multiple comparisons using the Holm-Bonferroni method.

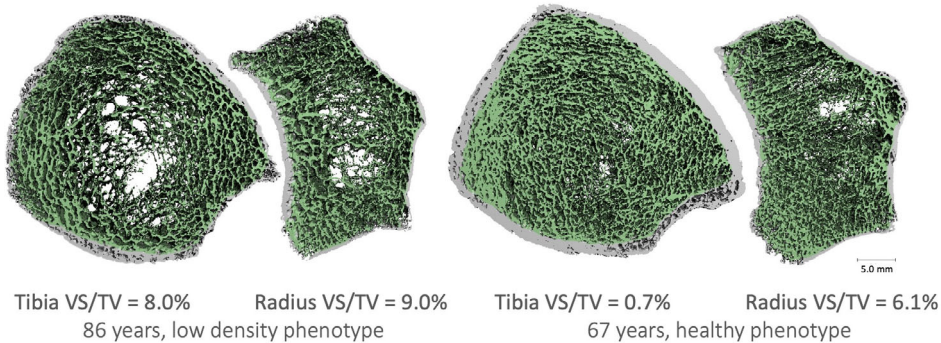
The algorithm was developed using bone parameters obtained on the first-generation HR-pQCT (XtremeCT, Scanco Medical), so consequently the second-generation data from this study could not be directly input. To account for differences between

first- and second-generation HR-pQCT systems, all HR-pQCT scans from hip fracture and control scans were cropped to 110 slices and downscaled from 61 μm to 82 μm to match the equivalent scan region and resolution obtained by first-generation HR-

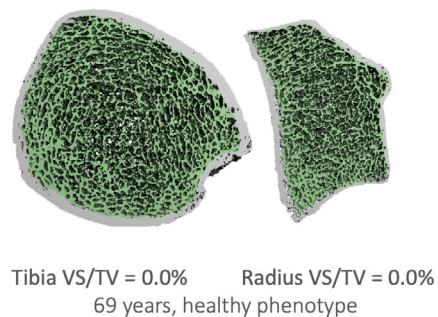
## Female hip fractures



## Male hip fractures



## Female control



## Male control

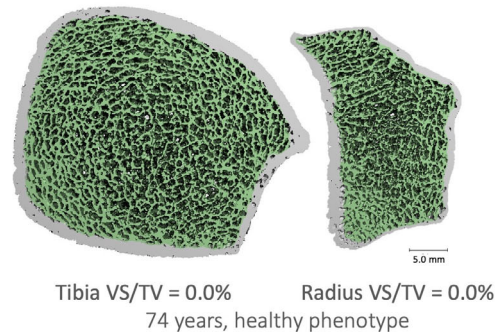


**Fig. 2.** Three-dimensional segmentations of representative tibia and radius HR-pQCT scans of hip fracture patients and healthy controls, with participant age and phenotype classification provided for each example. The cortical bone is colored in gray and trabecular bone colored in green.

pQCT (specifications provided in Supplemental Table S1 and Supplemental Fig. S1). The standard analysis for first-generation HR-pQCT was performed on the downscaled images, and using the previously developed phenotyping algorithm,<sup>(22)</sup> each participant was assigned a membership strength from 0 (no association) to 1 (complete association) with each of the three bone microarchitecture phenotypes, termed *low density*, *low volume*, and *healthy bone* phenotypes. Participants were classified into the phenotype with which they had the highest membership strength.

### Statistical analysis

Descriptive statistics were reported using mean and standard deviations (SD). Differences between hip fracture and control

groups for continuous parameters were compared using independent *t* test or Wilcoxon rank sum test depending on the data distribution, and differences in categorical parameters were assessed using the Fisher exact test. Bilateral comparisons of HR-pQCT tibia parameters were tested for significance using paired-samples *t* tests or Wilcoxon signed-rank test depending on the data distribution. Correlation between the change in hip fracture patients' mobility score pre- and post-fracture with bilateral differences in HR-pQCT parameters was tested using a Kendall's rank correlation test. All descriptive statistics and bilateral comparisons were adjusted for multiple comparisons using the Holm-Bonferroni method.

Logistic regression analysis was performed to estimate the association between fracture status and individual HR-pQCT bone parameters. The odds ratios (OR) with 95% confidence

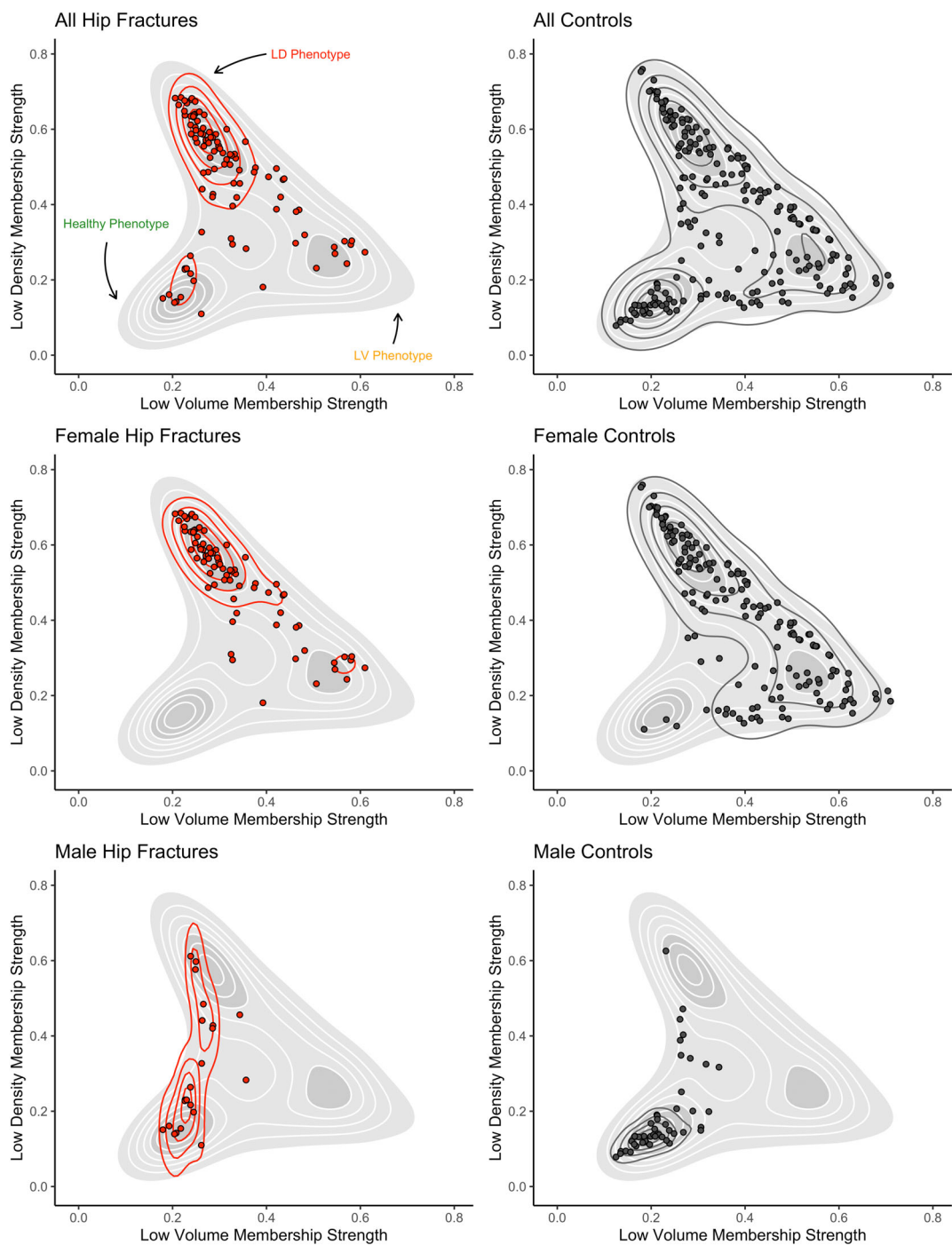


**Fig. 3.** Distribution of hip fractures (red, left) and controls (black, right) across bone microarchitecture phenotypes. The bone phenotype spectrum is shown as the area in light grey, and white topography lines indicating the typical population distribution across phenotypes. The focal points of the *low density* (LD), *low volume* (LV), and *healthy bone* phenotype regions are annotated in the top left panel. The red and black topography profiles indicate the density distribution of hip fracture and control subjects, respectively, across the phenotypes.

intervals (CI) were computed per 20-percentile point change in age- and sex-specific percentile values of HR-pQCT parameters.<sup>(23)</sup> The ORs were additionally tested with adjustment for FN aBMD. The scaling of ORs to per 20-percentile change was selected, rather than reporting in per SD (the conventional approach), as this is a more appropriate method to standardize

ORs across HR-pQCT parameters, and allows for direct comparison of results in future studies that use the same percentile scale. Age- and sex-specific percentiles are not available for VS/TV, so ORs were scaled to per 3 percentage-point increase in VS/TV, which is approximately equivalent to 1 SD change in tibia VS/TV for this population. All statistical analysis was

performed in R (v4.0.2) and significance was set to  $p < 0.05$  for all statistical tests.

## Results

### Participant characteristics

A total of 108 hip fracture patients (77% female) with a mean age of  $72.7 \pm 8.7$  years were enrolled in the study. Of the patients screened through the FLS program, 1986 eligible hip fractures occurred (Fig. 1). The primary reason for exclusion of patients with eligible fractures was due to declining physical or cognitive health ( $n = 845$ , 43%). The mean time between the hip fracture event and study visit was  $19.2 \pm 6.2$  weeks. Descriptive characteristics of hip fracture patients and controls are summarized in Table 1. The two groups did not differ significantly in terms of ethnicity, height, weight, prior fracture history, or current use of osteoporosis medications.

### Bilateral differences in hip fracture patients

Bilateral HR-pQCT tibia scans obtained from a subset of hip fracture patients ( $n = 65$ ) showed that side-to-side differences were not significant for all parameters except Tt.BMD, Ct.BMD, Ct.Ar, and failure load, and bilateral differences for these parameters were small (3% to 6%) and four to six times lower in magnitude

than differences observed between groups (Supplemental Fig. S2, Supplemental Table S3). Among hip fracture patients, the median and interquartile range (IQR) of mobility scores post-fracture was 2.0 (IQR: 1.0–3.0) at the time of study visit, indicative of occasional use of a walking aid for most patients. In addition, there were no significant correlations between a patient's change in mobility score pre- to post-fracture and bilateral differences in bone parameters at the tibias (Supplemental Table S2).

### Bone microarchitecture and phenotypes

Groupwise comparisons between hip fracture patients and controls for all bone-related parameters are presented in Table 2, and sex-stratified differences are provided in Supplemental Tables S3 and S4. Only 31% of hip fracture patients had a FN aBMD in the osteoporotic range ( $T\text{-score} \leq -2.5$ ), and the majority (62%) were classified as having low bone mass ( $-2.5 < T\text{-score} < -1.0$ ). The frequency of people with hip fractures classified in the low bone mass range and controls did not differ significantly, but on average hip fracture patients had 16% lower FN aBMD than controls ( $p < 0.01$ ).

All HR-pQCT parameters were significantly different between hip fractures and controls, with the exception of cross-sectional areas at both skeletal sites and Tb.Th, Ct.Th, and Ct.Po at the radius. The magnitude of differences between groups was

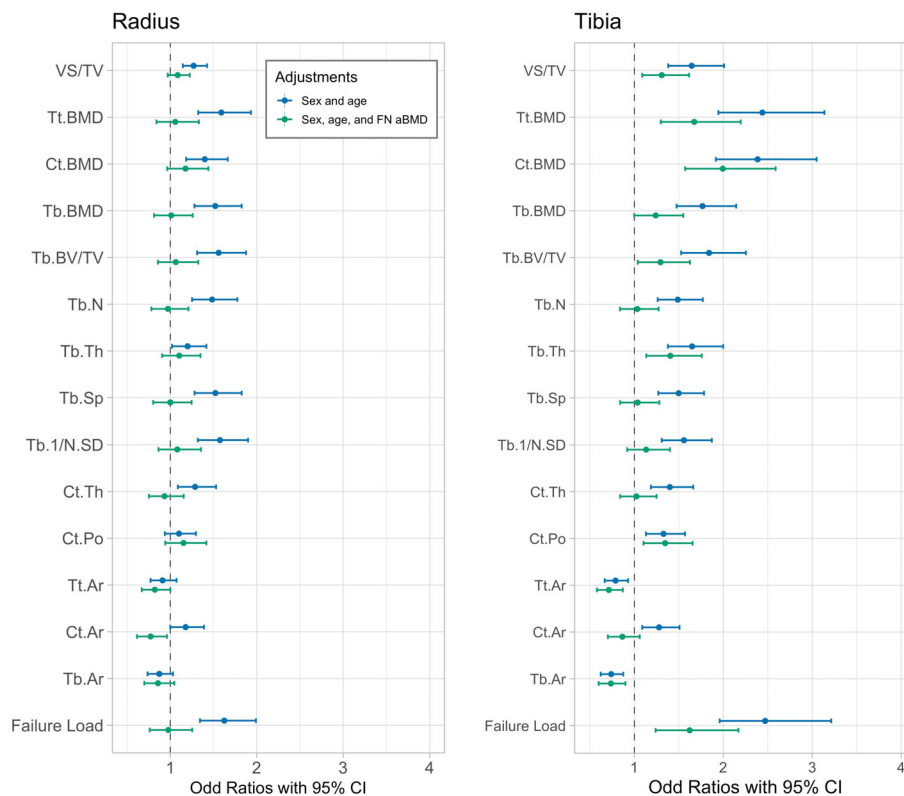


**Fig. 4.** Odds ratios and 95% confidence intervals (CI) between hip fracture and individual HR-pQCT parameters. All parameters are per 20-percentile decrease, except Tb.Sp, Tb.1/N.SD, and Ct.Po, which are per 20-percentile increase, and VS/TV, which is per 3 percentage-point increase. VS/TV = void space-to-total volume ratio; Tt.BMD = total BMD; Ct.BMD = cortical BMD; Tb.BMD = trabecular BMD; Tb.BV/TV = trabecular bone volume fraction; Tb.N = trabecular number; Tb.Th = trabecular thickness; Tb.Sp = trabecular separation; Tb.1/N.SD = trabecular inhomogeneity; Ct.Th = cortical thickness; Ct.Po = cortical porosity; Tt.Ar = total cross-sectional area; Ct.Ar = cortical cross-sectional area; Tb.Ar = trabecular cross-sectional area.

higher at the tibia than the radius for all parameters (Table 2). The largest groupwise differences were observed in VS/TV at the tibia and radius, where void spaces were two to four times larger on average in hip fracture patients than controls. In addition, hip fracture patients were significantly more likely to have void spaces at both HR-pQCT scan sites (Fig. 2).

In terms of phenotypic characteristics, hip fracture patients were predominantly associated with the *low density* phenotype (Fig. 3A, Table 2), with a significantly higher proportion of hip fracture patients (69%) classified in the *low density* phenotype relative to controls (40%). When stratified by sex, distributions across phenotypes differed; nearly all female hip fracture patients (78%) were classified in the *low density* phenotype (Fig. 3B, Supplemental Table S4), whereas the majority of males with hip fractures (64%) were classified in the *healthy bone* phenotype (Supplemental Table S5). However, when phenotypes are treated as continuous parameters (ie, using membership strengths), males with hip fractures had a significantly ( $p < 0.01$ ) higher membership strength to the *low density* phenotype ( $0.31 \pm 0.16$ ) when compared with controls ( $0.19 \pm 0.12$ ). This highlights that even if male hip fracture patients are classified categorically to be in the *healthy bone* phenotype, their bone characteristics appear to shift toward the *low density* group (Fig. 3C).

### Bone properties and fracture association

The logistic regression models, reported as sex- and age-adjusted ORs, showed that all HR-pQCT parameters were significantly associated with fracture risk, with the exception of cross-sectional areas at the radius and Ct.Po at the radius (Fig. 4, Supplemental Table S5). The ORs for decline in BMD and microarchitecture parameters were higher at the tibia (OR = 1.33–2.47) than the radius (OR = 1.18–1.62), indicating a stronger association between hip fracture risk and tibia bone characteristics. Conversely, ORs for cross-sectional areas at the tibia showed that a decrease in Tt.Ar and Tb.Ar was associated with a lower hip fracture risk (OR = 0.79 and 0.74). After adjustment for FN aBMD, all ORs at the radius were no longer associated with hip fracture, but at the tibia most parameters remained significantly associated, including BMD parameters, Tb.BV/TV, Tb.Th, Ct.Po, Tt.Ar, Tb.Ar, failure load, and VS/TV. Although the trabecular bone microarchitecture parameters capturing structural bone quality (Tb.Sp, Tb.N, and Tb.1/N.SD) at the tibia were no longer significant after adjustment, VS/TV remained significantly associated with fracture.

## Discussion

In this case-control study, we found that hip fracture patients had notable deterioration of bone microarchitecture and loss of BMD compared with healthy controls, especially at weight-bearing sites (tibia and femoral neck). Void spaces were more prevalent in hip fracture patients and were notably larger in size when compared with controls, especially at the tibia. Phenotypic analysis revealed that hip fracture patients were significantly associated with the *low density* bone phenotype when compared with controls. However, female and male hip fracture patients had distinctly different distributions across the bone phenotypes, indicating that sex-specific metrics or thresholds may be more effective for assessing patient-specific fracture risk. For instance, the male hip fracture patients were predominantly found in the *healthy bone* phenotype when discrete

classifications were considered, but male hip fracture patients had significantly higher association to the *low density* phenotype when compared with sex- and age-matched controls. The term “*healthy bone*” phenotype was chosen because of the above-average characteristics in bone properties observed for this group but should not be interpreted as all-encompassing in terms of bone health or fracture risk. The bone phenotypes are based on information captured by standard HR-pQCT measures, which provides extensive information on bone characteristics but is not exhaustive in capturing all attributes that determine bone health, such as the manifestation of void spaces (a new HR-pQCT measure), or tissue-level organization of the extracellular matrix. Although phenotyping may not capture exhaustive information about bone health, the OR analysis reinforced the insight gained with bone phenotyping, revealing that BMD parameters (primarily Tt.BMD and Ct.BMD at the tibia), which were previously identified as imaging biomarkers of fracture for the *low density* phenotype,<sup>(22)</sup> were of highest importance in differentiating hip fractures from controls. These findings suggest that the combination of bone characteristics associated with the *low density* phenotype predispose an individual to higher risk of hip fracture, and thus stratifying the population based on bone phenotypes alongside using phenotype-specific imaging biomarkers could be incorporated into future fracture prediction models to improve patient-specific assessment of fracture risk.

A strength of this work is the large sample size of patients with hip fractures that includes both male and female participants. Our groupwise differences and ORs were comparable to the reported findings in previous studies investigating female hip fracture populations,<sup>(17–19)</sup> and our current analysis adds assessment of  $\mu$ FE analysis, void space analysis, and bone phenotyping. In comparison to prior meta-analysis and prospective studies investigating fragility fracture risk (with skeletal sites pooled together), the overall trend of reduced BMD and deterioration of bone microarchitecture observed in fracture populations is consistent.<sup>(15,16)</sup> However, the association of certain parameters, such as Ct.Th, cross-sectional areas, and relative importance of the radius versus tibia in predicting fracture has been conflicting across several studies.<sup>(13,31–34)</sup> We expect this is a result of distinct patterns of bone characteristics, or bone phenotypes, that predispose individuals to higher risk of certain types of fracture. For example, in this study, larger Tt.Ar and Tb.Ar were associated with increased fracture risk, even after adjustment for FN aBMD. This may be a counterintuitive outcome, as higher cross-sectional areas typically correlate with higher bone strength, theoretically leading to lower fracture risk. The large prospective BoMIC study found that lower cross-sectional area was associated with higher fracture risk when all fracture sites are considered,<sup>(16)</sup> whereas the study by Zhu and colleagues found that a larger cross-sectional area is associated with increased hip fracture risk in females.<sup>(17)</sup> These contradictions can be elucidated when presented in the context of bone phenotypes.<sup>(22)</sup> The *low volume* phenotype has notably smaller cross-sectional area but thicker and denser cortical bone. In contrast, the *low density* phenotype has a larger cross-sectional area comparable to the *healthy bone* phenotype but with reduced overall BMD and thinner cortices. Both the *low volume* and *low density* phenotypes have higher risk of fracture when any site is considered, but in the present study, only the *low density* phenotype was associated with hip fracture risk, resulting in a positive correlation between cross-sectional area and fracture. The reason for the differences in fracture risk between phenotypes requires further investigation, but it is possible that the thicker, denser cortical



bone of the *low volume* phenotype provides some protection against fracture at cortical-dominant skeletal sites (ie, femoral neck), while susceptibility to fracture in general remains high due to trabecular bone loss. This distinction between phenotypes could have important clinical implications, as hip fractures are the primary outcome of concern when determining who should receive pharmacological treatment for osteoporosis.

Deficits in BMD and bone microarchitecture were found systemically in hip fracture patients, but after adjusting for FN aBMD, we found that only parameters at the tibia provided independent associations with fracture. In particular, Ct.BMD had the strongest association; however, characteristics that reflected considerable deterioration of bone microarchitecture, including VS/TV, Tb.Th, and Ct.Po, also remained significantly associated with hip fracture. Interestingly, VS/TV was a predictor of hip fracture risk independently of FN aBMD, even though conventional microarchitectural parameters that are meant to capture structural heterogeneity did not remain significant after adjustment (Tb.N, Tb.Sp, and Tb.1/N.SD). This may indicate that VS/TV is more sensitive in identifying structural deficits in bone microarchitecture that are related to biomechanical instability but are not entirely detected by global bone microarchitecture properties.

Our study is limited to retrospective assessment of bone characteristics associated with hip fracture. Prospective studies are optimal to determine truly predictive parameters, but this approach is not feasible because of the lower prevalence of hip fractures relative to other fracture sites.<sup>(3,6)</sup> We were concerned with this limitation, which is why we investigated whether asymmetric bone loss occurred at the tibiae due to unloading after fracture. Although some bilateral differences were observed, these were four to six times lower in magnitude than the differences observed between hip fracture cases and controls. In addition, long-term changes in mobility due to fracture were relatively small in terms of the self-reported mobility scores provided, and there was no association observed between the magnitude of change in patient mobility and bilateral differences at the tibia ( $p = 0.99$ ). This near-full recovery in mobility among enrolled hip fracture patients highlights the selection bias toward healthier patients that are more likely to recover. The majority of eligible patients screened (Fig. 1) were not sufficiently healthy to participate in the study and likely have reduced bone quality, suggesting that differences between hip fracture patients and controls could be far larger than what was captured in this study. Another factor that is expected to influence bone measurements was the use of osteoporosis medications. Although no significant differences were found between hip fractures and controls in terms of current medication, we cannot completely exclude the possibility that medications had an impact on bone.

The recently introduced approach for bone phenotyping was based on first-generation HR-pQCT, and so we downscaled our data to convert second-generation to first-generation HR-pQCT, which likely causes some measurement errors. Although BMD parameters are resolution-independent, some structural parameters such as Ct.Th and Tb.N are less robust to conversion across generations.<sup>(35)</sup> These differences may have led to variance in some individual measurements; however, the impact on phenotyping, which relies on numerous measures at both scan sites, is expected to be minimal. Given the improvements of second-generation HR-pQCT, there is a need to establish large population-based prospective cohorts, similar to what has been established by the BoMIC consortium, but this will take time to establish and likely requires an internationally coordinated effort.

In summary, compared with controls, hip fracture patients had highly heterogeneous microarchitectural deterioration, as shown using void space analysis. The added benefit of HR-pQCT is highlighted by bone phenotyping, where systemic structural features associated to hip fracture in males and females were identified, providing insight to the underlying mechanisms of bone fragility.

## Disclosures

---

All authors state that they have no conflicts of interest.

## Acknowledgments

---

The authors thank all the individuals who gave their time to participate in this study; the Fracture Liaison Services for their instrumental support in screening and recruiting patients; Michelle Kan, Jane Allan, and Jolene Allan for participant intake and data collection; and Anne Cooke and Stephanie Kwong for scan acquisition. Research reported in this publication was supported by the Canadian Institutes of Health Research (#364554). Additionally, Danielle E. Whittier received funding support from the Biomedical Engineering Graduate Program at the University of Calgary and the Natural Sciences and Engineering Research Council of Canada.

## Author Contributions

---

**Danielle E. Whittier:** Conceptualization; data curation; formal analysis; investigation; methodology; validation; visualization; writing – original draft; writing – review and editing. **Sarah L. Manske:** Conceptualization; funding acquisition; investigation; project administration; writing – review and editing. **Emma Billington:** Formal analysis; funding acquisition; investigation; writing – review and editing. **Richard E. A. Walker:** Funding acquisition; investigation; writing – review and editing. **Prism S. Schneider:** Investigation; resources; supervision; writing – review and editing. **Lauren A. Burt:** Data curation; investigation; project administration; validation; writing – review and editing. **David A. Hanley:** Conceptualization; funding acquisition; investigation; writing – review and editing. **Steven K. Boyd:** Conceptualization; funding acquisition; investigation; methodology; resources; supervision; validation; writing – review and editing.

## Peer Review

---

The peer review history for this article is available at <https://publons.com/publon/10.1002/jbmr.4663>.

## Data Availability Statement

---

The population data sets analyzed during the current study are not publicly available to protect confidentiality and privacy of participants but may be made available from the corresponding author on reasonable request.

## References

---

1. Morin S, Lix LM, Azimae M, Metge C, Majumdar SR, Leslie WD. Institutionalization following incident non-traumatic fractures in community-dwelling men and women. *Osteoporos Int.* 2012;23(9):2381-2386.

2. Tarride JE, Burke N, Leslie WD, et al. Loss of health related quality of life following low-trauma fractures in the elderly. *BMC Geriatr.* 2016;16:84.
3. NIH Consensus Development Panel on Osteoporosis Prevention, Diagnosis, and Therapy, March 7-29, 2000: highlights of the conference. *South Med J.* 2001;94(6):569-573.
4. Cauley JA, Thompson DE, Ensrud KC, Scott JC, Black D. Risk of mortality following clinical fractures. *Osteoporos Int.* 2000;11(7):556-561.
5. Sernbo I, Johnell O. Consequences of a hip fracture: a prospective study over 1 year. *Osteoporos Int.* 1993;3(3):148-153.
6. Tarride JE, Hopkins RB, Leslie WD, et al. The burden of illness of osteoporosis in Canada. *Osteoporos Int.* 2012;23(11):2591-2600.
7. NIH Panel. NIH Consensus Development Panel on Osteoporosis Prevention, Diagnosis, and Therapy: osteoporosis prevention, diagnosis, and therapy. *JAMA.* 2001;285(6):785-795.
8. Siris ES, Chen YT, Abbott TA, et al. Bone mineral density thresholds for pharmacological intervention to prevent fractures. *Arch Intern Med.* 2004;164(10):1108-1112.
9. Gourlay ML, Overman RA, Fine JP, et al. Time to osteoporosis and major fracture in older men: the MrOS study. *Am J Prev Med.* 2016;50(6):727-736.
10. Schuit SC, van der Klift M, Weel AE, et al. Fracture incidence and association with bone mineral density in elderly men and women: the Rotterdam study. *Bone.* 2004;34(1):195-202.
11. Kanis JA, Oden A, Johansson H, Borgstrom F, Strom O, McCloskey E. FRAX and its applications to clinical practice. *Bone.* 2009;44(5):734-743.
12. Kanis JA, Johnell O, Oden A, Johansson H, McCloskey E. FRAX and the assessment of fracture probability in men and women from the UK. *Osteoporos Int.* 2008;19(4):385-397.
13. Boutroy S, Bouxsein ML, Munoz F, Delmas PD. In vivo assessment of trabecular bone microarchitecture by high-resolution peripheral quantitative computed tomography. *J Clin Endocrinol Metab.* 2005;90(12):6508-6515.
14. van den Bergh JP, Szulc P, Cheung AM, Bouxsein M, Engelke K, Chapurlat R. The clinical application of high-resolution peripheral computed tomography (HR-pQCT) in adults: state of the art and future directions. *Osteoporos Int.* 2021;32(8):1465-1485.
15. Mikolajewicz N, Bishop N, Burghardt AJ, et al. HR-pQCT measures of bone microarchitecture predict fracture: systematic review and meta-analysis. *J Bone Miner Res.* 2020;35(3):446-459.
16. Samelson EJ, Broe KE, Xu H, et al. Cortical and trabecular bone microarchitecture as an independent predictor of incident fracture risk in older women and men in the Bone Microarchitecture International Consortium (BoMIC): a prospective study. *Lancet Diabetes Endocrinol.* 2019;7(1):34-43.
17. Zhu TY, Hung VW, Cheung WH, Cheng JC, Qin L, Leung KS. Value of measuring bone microarchitecture in fracture discrimination in older women with recent hip fracture: a case-control study with HR-pQCT. *Sci Rep.* 2016;6:34185.
18. Sundh D, Nilsson AG, Nilsson M, Johansson L, Mellstrom D, Lorentzon M. Increased cortical porosity in women with hip fracture. *J Intern Med.* 2017;281(5):496-506.
19. Vico L, Zouch M, Amirouche A, et al. High-resolution pQCT analysis at the distal radius and tibia discriminates patients with recent wrist and femoral neck fractures. *J Bone Miner Res.* 2008;23(11):1741-1750.
20. Manske SL, Zhu Y, Sandino C, Boyd SK. Human trabecular bone microarchitecture can be assessed independently of density with second generation HR-pQCT. *Bone.* 2015;79:213-221.
21. Whittier DE, Burt LA, Boyd SK. A new approach for quantifying localized bone loss by measuring void spaces. *Bone.* 2021;143:115785.
22. Whittier DE, Samelson EJ, Hannan MT, et al. Bone microarchitecture phenotypes identified in older adults are associated with different levels of osteoporotic fracture risk. *J Bone Miner Res.* 2022;37(3):428-439.
23. Whittier DE, Burt L, Hanley DA, Boyd S. Sex- and site-specific reference data for bone microarchitecture in adults measured using second-generation HR-pQCT. *J Bone Miner Res.* 2020;35(11):2151-2158.
24. Bowers TM, Parker MJ. Assessment of outcome after hip fracture: development of a universal assessment system for hip fractures. *SICOT J.* 2016;2:27.
25. Whittier DE, Boyd SK, Burghardt AJ, et al. Guidelines for the assessment of bone density and microarchitecture in vivo using high-resolution peripheral quantitative computed tomography. *Osteoporos Int.* 2020;31(9):1607-1627.
26. Pauchard Y, Liphardt AM, Macdonald HM, Hanley DA, Boyd SK. Quality control for bone quality parameters affected by subject motion in high-resolution peripheral quantitative computed tomography. *Bone.* 2012;50(6):1304-1310.
27. Buie HR, Campbell GM, Klinck RJ, MacNeil JA, Boyd SK. Automatic segmentation of cortical and trabecular compartments based on a dual threshold technique for in vivo micro-CT bone analysis. *Bone.* 2007;41(4):505-515.
28. Whittier DE, Mudryk AN, Vandergaag ID, Burt LA, Boyd SK. Optimizing HR-pQCT workflow: a comparison of bias and precision error for quantitative bone analysis. *Osteoporos Int.* 2020;31(3):567-576.
29. Whittier DE, Manske SL, Kiel DP, Bouxsein M, Boyd SK. Harmonizing finite element modelling for non-invasive strength estimation by high-resolution peripheral quantitative computed tomography. *J Biomech.* 2018;80:63-71.
30. Pistoia W, van Rietbergen B, Lochmuller EM, Lill CA, Eckstein F, Rueggsegger P. Estimation of distal radius failure load with micro-finite element analysis models based on three-dimensional peripheral quantitative computed tomography images. *Bone.* 2002;30(6):842-848.
31. Stein EM, Liu XS, Nickolas TL, et al. Abnormal microarchitecture and reduced stiffness at the radius and tibia in postmenopausal women with fractures. *J Bone Miner Res.* 2010;25(12):2572-2581.
32. Boutroy S, Khosla S, Sornay-Rendu E, et al. Microarchitecture and peripheral BMD are impaired in postmenopausal white women with fracture independently of total hip T-score: an international multicenter study. *J Bone Miner Res.* 2016;31(6):1158-1166.
33. Szulc P, Boutroy S, Vilayphiou N, Chaitou A, Delmas PD, Chapurlat R. Cross-sectional analysis of the association between fragility fractures and bone microarchitecture in older men: the STRAMBO study. *J Bone Miner Res.* 2011;26(6):1358-1367.
34. Langsetmo L, Peters KW, Burghardt AJ, et al. Volumetric bone mineral density and failure load of distal limbs predict incident clinical fracture independent HR-pQCT BMD and failure load predicts incident clinical fracture of FRAX and clinical risk factors among older men. *J Bone Miner Res.* 2018;33(7):1302-1311.
35. Manske SL, Davison EM, Burt LA, Raymond DA, Boyd SK. The estimation of second-generation HR-pQCT from first-generation HR-pQCT using in vivo cross-calibration. *J Bone Miner Res.* 2017;32(7):1514-1524.